Chinese Chemical Letters 36 (2025) 109811

Contents lists available at ScienceDirect

Chinese Chemical Letters

journal homepage: www.elsevier.com/locate/cclet

Full biosynthetic pathway of pyrrolobenzoxazines

Kunya Wang, Bingyu Liu, Daojiang Yan, Jian Bai, Haibo Yu, Youcai Hu*

State Key Laboratory of Bioactive Substance and Function of Natural Medicines, Institute of Materia Medica, Chinese Academy of Medical Sciences & Peking Union Medical College, Beijing 100050, China

ARTICLE INFO

Article history:
Received 14 February 2024
Revised 18 March 2024
Accepted 21 March 2024
Available online 22 March 2024

Keywords:
Pyrrolobenzoxazines
Paeciloxazine
Biosynthesis
P450 monooxygenase
Antiepileptic activity

ABSTRACT

Pyrrolobenzoxazines are a rare terpene-amino acid family of natural products with potent biological activities. Here, we reported the full biosynthetic pathway of paeciloxazine (**1**), a typical pyrrolobenzoxazine, with significant insecticidal activity. Base on heterologous expression, chemical complement experiment, and *in vitro* biochemical assays, we demonstrated the sesquiterpene portion of **1** derived from discontinuously oxidations of amorphdiene, in which P450 monooxygenase PaxH catalyzed a cascade of hydroxylation and epoxidation, while two flavin dependent monooxygenases are involved in the transformation of the esterified tryptophan into a pyrrolobenzoxazine core. Furthermore, a total of 15 compounds were generated through heterologous expression, of which **13**, **17** and **20** showed potential antiepileptic activity. This study fully elucidated the biosynthetic pathway of paeciloxazine (**1**) and showed the diversity and complexity of constructing natural products by organisms.

The diversity of chemical structures of active natural products, which are the focus of innovative drug research [1], have spurred interest in nature's chemical strategy to produce complexity [2–4]. The biosynthetic pathways of natural products employ powerful chemical concepts to more concise and efficient [2], including convergent synthesis [5], oxidative cyclization [6], and cascade reactions [7]. Thus, uncovering the enzymatic basis of biosynthesis could improve complexity generation strategies and increases the toolbox of biocatalysts used to generate structural diversity.

Pyrrolobenzoxazines are a hybrid terpene-amino acid natural product family [8–13], in which a rare pyrrolobenzoxazine core is esterified to a heavily oxidized juniper-type sesquiterpene. This characteristic of fusion of different fragment families is exemplary of the complexity generation strategy used by nature. The pyrrolobenzoxazines are however rare, with eight examples (Fig. 1) [8–13], and the majority of these products have been shown to have potent biological activities [8-10,13-17]. For example, paeciloxazine (**1**), which was first isolated from the fungus *Paecilomyces* BAUA3058, was reported to show significant insecticidal activity [8]. CJ-12662 and CJ-12663 which was isolated from *Aspergillus fischeri* var. *thermomutatus* ATCC 18618, shows remarkable antiparasitic activity [10].

The unique scaffold of pyrrolobenzoxazines has led to several studies of total synthesis [11,18-20]. While the biosynthesis of pyrrolobenzoxazines is rarely reported, in our previous study, we identified the biosynthetic gene cluster of **1** from *Penicillium janthinellum*, and elucidated the mechanism that flavin dependent monooxygenase PaxA catalyzed the construction of 1,2-oxazine in **1** *via* Meisenheimer rearrangement [12]. Here, we continue to explore the full biosynthetic pathway of **1** and peniciloxazine A (**2**).

The *pax* cluster, which is responsible for the biosynthetic of **1**, contains 9 genes (*paxA–I*) coding for several functional proteins, including two P450 monooxygenases (PaxD and PaxH), two flavin dependent monooxygenases (PaxA and PaxF), a nonheme, iron and α-ketoglutarate dependent dioxygenase (PaxC), a methyltransferase (PaxB), an acyltransferase (PaxE), a mono-modular NRPS (PaxG), and a terpene cyclase (PaxI) (Fig. 2A, Fig. S1 in Supporting information).

Based on the structural features of **1** and **2**, we proposed that the terpene and the alkaloid portions are heavily oxidized by redox enzymes, and the sesquiterpene is a triply-oxygenated derivative of amorphadiene, which is the precursor of antimalarial artemisinin (Fig. S2 in Supporting information) [21]. Bioinformatic analysis showed PaxD, PaxH and PaxC encoded by the *pax* cluster share moderate similarity to sesquiterpene oxidase AneD (36%), AneG (41%), and AneA (53%), respectively (Fig. S3 in Supporting information) [12,22]. This indicates that PaxD, PaxC, and PaxH possibly function at the sesquiterpene moiety in **2**.

To elucidate the biosynthetic pathway of the sesquiterpene moiety in **1**/**2**, we constructed recombinant strains of *A. nidulans* expressing different combinations of genes *paxC/D/E/H/I*. When *paxC/I* or *paxD/I* were co-expressed in *A. nidulans*, no new metabolite was detected (Fig. 2B, traces iii and iv). While co-expression of

* Corresponding author.
E-mail address: huyoucai@imm.ac.cn (Y. Hu).

https://doi.org/10.1016/j.cclet.2024.109811
1001-8417/

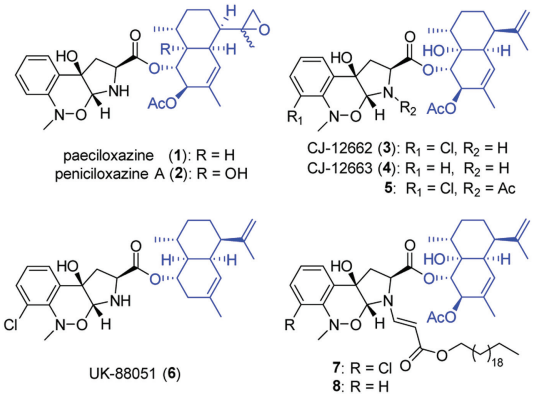

Fig. 1. The family of pyrrolobenzoxazine natural products.

paxH/I led to genenation of two additional metabolites **9** and **10** (Fig. 2B, trace ii). NMR characterization revealed the oxidation at C-2 and epoxidation at C-10/11 in the structures of **9** and **10**. We proposed that PaxH catalyzed the transformation of amorphadiene into **9**, which dehydrogenated to form **10** by the host. To confirm the function of PaxH, we fed amorphadiene into *Saccharomyces cerevisiae* expressing *paxH* (*SC-paxH*) and observed the generation of **9** (Fig. S4 in Supporting information). These results verified that P450 monooxygenase PaxH catalyze two-step oxidations, hydroxylation and epoxidation, at amorphadiene to form **9**.

With *paxH/I*, further expression of *paxC* did not lead to new metabolite, while adding the *paxD* led to formation of **11** (Fig. 2B, traces v–vi). The additional hydroxy group was assigned at C1 based on the HMBC correlations, which suggested PaxD was responsible for catalyzing hydroxylation at C1. In addition, when co-expressed *paxE/H/I* in *A. nidulans*, we observed the formation of **12**, which was confirmed to be 2-*O*-acetyl-**9** (Fig. 2B, trace vii). We proposed that acyltransferase PaxE catalyzed the conversion of **9** to **12**. To confirm the function of PaxE, we expressed and purified PaxE as a recombinant protein from *Escherichia coli* BL21 Transetta and directly performed *in vitro* assays in the presence of 2.3 μmol/L PaxE, 0.1 mol/L of acetyl-CoA and 0.1 mmol/L of substrates (**9** or **10**). Liquid chromatograph-mass spectrometer (LC-MS) analysis showed that the purified PaxE converted **9** and **11** to **12** and **14**, respectively (Fig. S5 in Supporting information). In order to further confirm the natural substrate of PaxE, we performed *in vitro* reaction using low concertation of PaxE (0.1 μmol/L) with **9** and **11** at a ratio of 1:1 as substrate, which showed that only **9** was converted to **12** (Fig. S6 in Supporting information). This result highly suggested **9** as the preferred substrate of PaxE. Then we separately fed amorphadiene, **9**, **12**, and **13** into *S. cerevisiae* expressing *paxD* (*SC-paxD*) to identify the role of PaxD. Although feeding amorphadiene did not lead to new metabolite, the transformation of **9**, **12**, and **13** into **11**, **14**, and **16**, respectively, was observed (Fig. S7 in Supporting information), which indicated that PaxD is the enzyme required for hydroxylation at C1 and the formation of C1-OH happened after oxidation at C-2. Furthermore, we performed *in vitro* assays using reactions containing PaxD microsomes, 0.1 mol/L of NADPH, and 0.2 mmol/L of the substrate (**9**/**12**/**13**) and observed that only **12** was converted to **14** (Fig. S8 in Supporting information). These highly suggested that the natural substrate of PaxD was **12**. We speculated that activity of PaxD in microsome was weak in the *in vivo* assay, resulting in inability of conversion of non-natural substrates.

We proposed the next step to form the terpene fragment is hydroxylation at C-8a. Co-expression of *paxC/D/E/H/I* in *A. nidulans* led to the generation of **15**, suggesting that PaxC was responsible for the hydroxylation at C-8a (Figs. 2B and C). Furthermore, we also detected the formation of **16** and **17**, which were derived from the hydration and acetylation of **14**, respectively. To confirm the function of PaxC, we then expressed and purified the recombinant PaxC from *E. coli* BL21, and initially performed *in vitro* assays using reactions containing 100 μmol/L of purified PaxC, 1 mmol/L $FeSO_4$, 10 mmol/L α-ketoglutarate (α-KG) and 0.1 mmol/L of the substrate (amorphadiene, **9**, **11**, **12**, or **14**, separately). The transformation from **12** and **14** to **12a** and **15**, respectively, was observed (Fig. S9 in Supporting information), which indicates that hydroxylation at C-8a was catalyzed by PaxC. While the failure of PaxD in conversion of **12a** to **15**, highly suggested that **12a** was a shunt product (Figs. S7 and S8). In addition, the incomplete consumption of **14** at

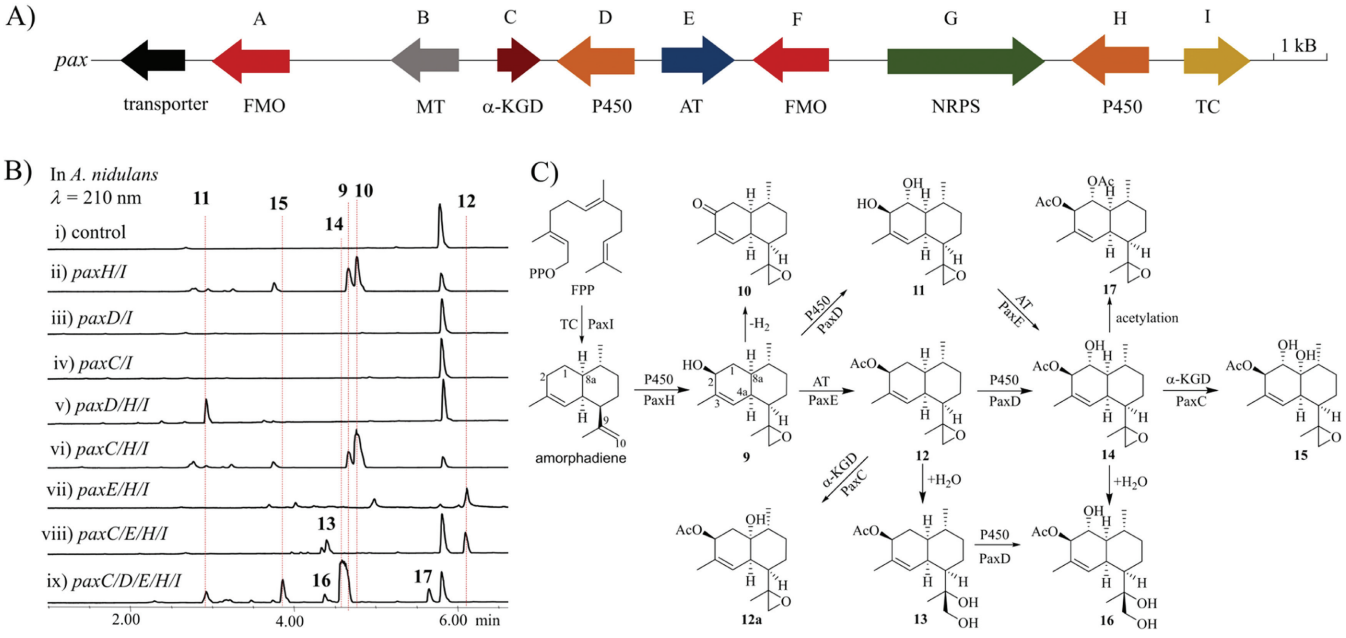

Fig. 2. Biosynthesis of sesquiterpene moiety in **2**. (A) The *pax* gene cluster from *P. janthinellum*. (B) LC-MS analysis of metabolites produced by *A. nidulans* transformed with different combinations of *pax* genes. (C) Biosynthetic pathway from farnesyl diphosphate (FPP) to **15**.

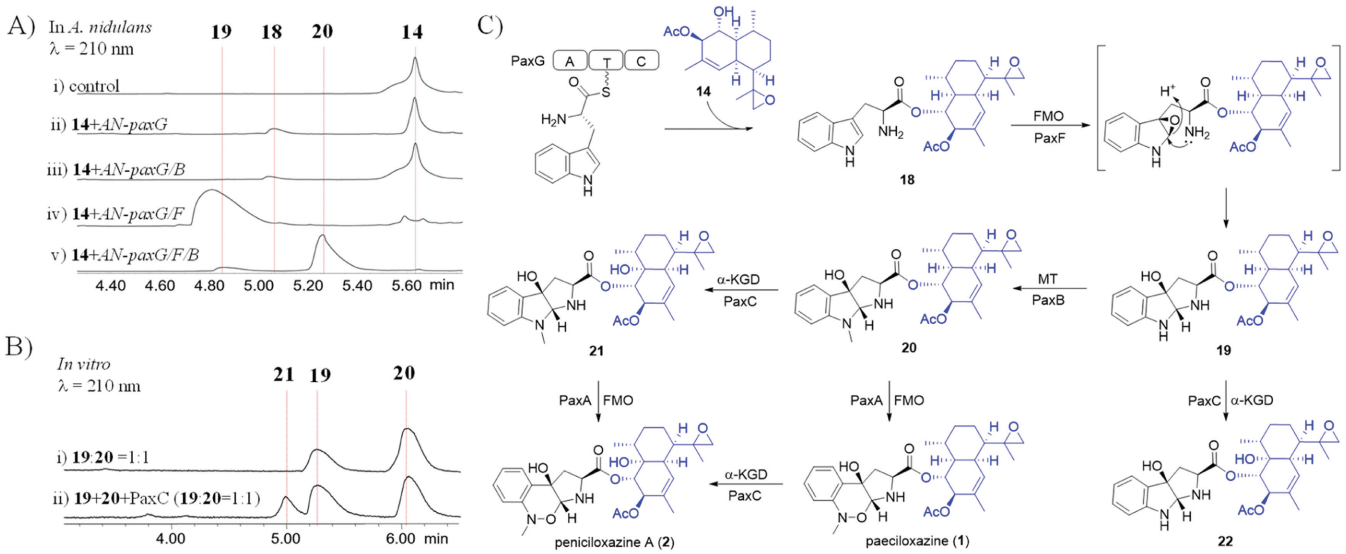

Fig. 3. Biosynthesis of pyrrolobenzoxazine core of **2**. (A) LC-MS analysis of chemical remediation experiment of **14**. (B) LC traces from *in vitro* assays of PaxC activity. Reaction conditions: 0.1 mmol/L substrate, 0.1 μmol/L PaxC, 1 mmol/L $FeSO_4$, 10 mmol/L α-KG and 50 mmol/L Tris–HCl buffer (pH 7.9), 20 °C for 5 min. (C) Biosynthetic pathway from **14** to **1** and **2**. Blue marks: terpene moiety; black marks: alkaloid portions.

the high concentration of PaxC, suggested that **14** may not be the natural substrate of PaxC.

Having established the pathway of the sesquiterpene fragments in **2**, we next tried to identify the pathways leading to the pyrrolobenzoxazine core. To identify the role of NRPS PaxG, compounds **11**, **14**, and **15** were separately fed to *A. nidulans* expressing *paxG* (*AN-paxG*) (Fig. 3A, Fig. S10 in Supporting information). While feeding **11** (or **15**) did not led to any new metabolites, feeding **14** led to the formation of **18**, an adduct of **14** and L-tryptophan (Fig. 3A, Fig. S10). These supported that PaxG function before PaxC which catalyze the hydroxylation at C-8a.

With **18** in hand, we next investigated the formation of the *N*-methylpyrroloindoline scaffold. Feeding of **14** to *A. nidulans* expressing *paxG/B* did not lead to any methylated indole products (Fig. 3A, trace iii), which suggested that the function of PaxB probably required the presence of pyrroleindole ring in the substrate. The remain oxidases, PaxA and PaxF, were clustered with the indole hydroxylase AspB [23] in phylogenetic analysis (Fig. S11 in Supporting information) and our previous study has identified PaxA as the enzyme responsible for the formation of 1,2-oxazine core [12], which suggested that PaxF could be a candidate enzyme to install the pyrroleindole core. Indeed, when **14** was fed to *A. nidulans* expressing *paxG/F* (*AN-paxG/F*), the generation of a new product **19** was observed (Fig. 3A, trace iv). NMR characterization revealed a pyrroleindole core in the structure of **19**. These results highly suggested PaxF responsible for installation of pyrroleindole moiety. Base on the enzymatic mechanism of homologues of PaxF, such as AspB [23], NotB [24], and CtdE [25] (Fig. S12 in Supporting information), a mechanism of PaxF catalyzing the formation of pyrroleindole core could be proposed. A first formation of 2,3-β-face epoxidation to facilitate α-amino attack at electrophilic C2 of the epoxyindole ring (Fig. 3C). Next, we fed **14** into the *AN-paxG/F/B* to identify the role of PaxB, and *N*-methylpyrroleindole product **20** was detected (Fig. 3A, trace v). These results indicated that the formation of pyrroleindole ring happened before *N*-methylation catalyzed by PaxB.

Previously, we have identified **21** as the natural substrate of PaxA, which suggested that hydroxylation at C-8′a occurred before the formation of 1,2 oxazine core [12]. To identify the natural substrate of PaxC, the *in vitro* reactions using low concertation (0.1 μmol/L) of PaxC with substrates (**14**/**18**/**19**/**20**) at 20 °C for 5 min were performed (Fig. S13 in Supporting information). When co-incubated with **14** and PaxC (0.1 μmol/L), the formation of C8′a-OH product **15** was not detected, which supported the above result of feeding **14** to *AN-paxG*. Then the compounds **18**, **19**, and **20** were separately add to *in vitro* assays of PaxC, and only the corresponding C-8′a hydroxylation products of **19** and **20** were detected. Furthermore, when a mixture of **19** and **20** (1:1 ratio) was used in the *in vitro* assay, **20** was firstly converted to **21** (Fig. 3B). Therefore, **20** was suggested as the natural substrate of PaxC.

Based on the results of heterologous expression, feeding experiment and *in vitro* biochemical assays, we established the complete biosynthetic pathway of paeciloxazine (**1**) and peniciloxazine A (**2**). Firstly, the terpene cyclase PaxI converts FPP to amorphadiene, which is converted to **9** catalyzed by the P450 monooxygenase PaxH through two-step oxidations, hydroxylation at C-2 and epoxidation at C-9/10. Next, **9** is transform into **12** catalyzed by acyltransferase PaxE, followed by the formation of C1-OH to obtain **14** catalyzed by PaxD. Then the esterification of L-tryptophan with **14** occurs in the presence of PaxG to form **18**, which is catalyzed by a FMO PaxF and methyltransferase PaxB in turn to form *N*-methypyrroleindole **20**. Then, **20** is converted to paeciloxazine (**1**) catalyzed by PaxA. Alternatively, **20** can also be converted to **21** by PaxC, following by the formation of **2** catalyzed by PaxA (Fig. S14 in Supporting information).

In all, the full biosynthetic pathway of **1** and **2** was established and 15 compounds were obtained by heterologous expression. In order to explore the potential applications of these on-pathway intermediates, **1**, **2**, **9**–**17**, **20** and **21** were evaluated for their inhibitory effect on epileptiform activity of 4-AP-induced synchronized calcium oscillations (SCOs), with the NMDA receptor inhibitor MK801 [26] as a positive control. Compounds **13**, **17**, and **20** showed significant activities of inhibiting calcium oscillation (Fig. 4), which suggested their potential antiepileptic activity.

During our investigation of the biosynthesis of **1**, Tang group reported the biosynthetic pathway of another pyrrolobenzoxazine compound CJ-12662 (Fig. S15 in Supporting information) [27]. Analysis of the biosynthetic pathways of CJ-12662 and peniciloxazine A (**2**) showcased the different strategies nature employs to generate similar nature product (Fig. S16 in Supporting information). First, the hydroxylation happened at C2, C1, and C8a in turn in the biosynthesis of paeciloxazine A (**2**), while happened at C1,

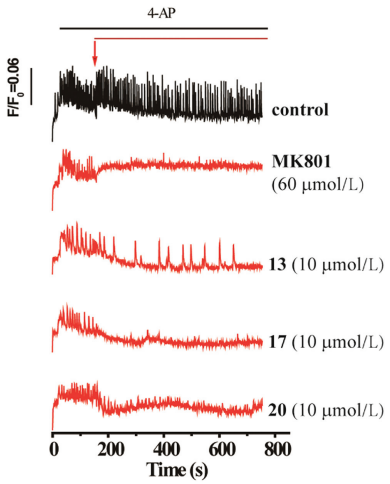

Fig. 4. Representative curves of inhibition of SCOs by the positive drugs MK801 and compounds **13**, **17**, and **20**. The arrows: vehicle control.

C2, and C8a in turn in CJ-12662. Contrast with the P450 monooxygenase ThmG in the biosynthesis of CJ-12662, which is responsible for C8a hydroxylation of dihydroxyl sesquiterpene, the α-KG dependent dioxygenase PaxC in biosynthesis of **2** catalyzes the C8a hydroxylation of an alkaloid-terpene substrate **20**. It is notable that different strategies were employed for acetylation during the biosynthesis of these two compounds. The acetylation requires the presence of polyketide synthase (PKS) ThmK and acyltransferase ThmJ in the biosynthesis of CJ-12662, whereas the acetylation is accomplished by acetyltransferase PaxE alone in the case of **2**. Different from ThmG that catalyzes the hydroxylation at C2, PaxH is responsible for the epoxidation at C9/10 besides the formation of C2-OH.

In summary, we fully elucidated the biosynthetic pathway of paeciloxazine (**1**), and revealed the diversity and complexity of constructing natural products by organisms. In addition, a total of 15 compounds were obtained by heterologous expression, of which compounds **13**, **17**, and **20** showed potential antiepileptic activities.

Declaration of competing interest

The authors declare that they have no known competing financial interests or personal relationships that could have appeared to influence the work reported in this paper.

CRediT authorship contribution statement

Kunya Wang: Data curation, Formal analysis, Investigation, Methodology, Validation, Writing – original draft. **Bingyu Liu:** Formal analysis, Funding acquisition, Investigation, Methodology. **Daojiang Yan:** Investigation, Methodology. **Jian Bai:** Methodology, Writing – review & editing. **Haibo Yu:** Investigation, Validation. **Youcai Hu:** Data curation, Funding acquisition, Project administration, Supervision, Validation, Writing – original draft, Writing – review & editing.

Acknowledgments

This work was supported financially by the National Natural Science Foundation of China (Nos. 22107122 and 82225042) and the CAMS Innovation Fund for Medical Sciences (CIFMS, No. 2021-I2M-1–029).

Supplementary materials

Supplementary material associated with this article can be found, in the online version, at doi:10.1016/j.cclet.2024.109811.

References

[1] D.J. Newman, M.C. Gordon, J. Nat. Prod. 83 (2020) 770–803.
[2] C.T. Walsh, Y. Tang, Natural Product Biosynthesis: Chemical Logic and Enzymatic Machinery, 1st. ed., The Royal Society of Chemistry, Croydon, 2017.
[3] W. Yuan, F. Li, Z. Chen, et al., Chin. Chem. Lett. 35 (2024) 108788.
[4] F. Jiang, A. Liu, Q. Wei, Y. Hu, Chin. Chem. Lett. 35 (2024) 109504.
[5] T. Dairi, T. Kuzuyama, M. Nishiyama, I. Fujii, Nat. Prod. Rep. 28 (2011) 1054–1086.
[6] M.C. Tang, Y. Zou, K. Watanabe, et al., Chem. Rev. 117 (2016) 5226–5333.
[7] C.T. Walsh, B.S. Moore, Angew. Chem. Int. Ed. 58 (2019) 6846–6879.
[8] K. Yoshinori, F. Tsukasa, S. Kochi, et al., J. Antibiot. 57 (2004) 24–28.
[9] D.A. Perry, H. Maede, J. Tone, Patent, GB2240100 A, 1991.
[10] Y. Kojima, H. Kaminawa, N. Aichiken, et al., Patent, WO 95/19363, 1995.
[11] C. Didier, D.J. Critcher, N.D. Walshe, et al., J. Org. Chem. 69 (2004) 7875–7879.
[12] D. Yan, K. Wang, S. Bai, et al., J. Am. Chem. Soc. 144 (2022) 4269–4276.
[13] B. Chaiyosang, K. Kanokmedhakul, K. Soytong, et al., Planta Med. 87 (2021) 600–610.
[14] K. Kanokmedhakul, S. Kanokmedhakul, R. Suwannatrai, et al., Tetrahedron 67 (2011) 5461–5468.
[15] J. Paluka, K. Kanokmedhakul, M. Soytong, et al., Fitoterapia 137 (2019) 104257.
[16] N.A.L. Chubb, D.J. Critcher, J.J. Eshelby, et al., Patent, WO 2004/072086, 2004.
[17] M. Masi, A. Andolfi, V. Mathieu, et al., Tetrahedron 69 (2013) 7466–7470.
[18] C. Commandeur, M. Commandeur, K. Bathany, et al., Tetrahedron 67 (2011) 9899–9908.
[19] D. Schwaebisch, K. Tchabanenko, R.M. Adlington, et al., Chem. Commun. 36 (2004) 2552–2553.
[20] B.K. Das, E. Tokunaga, K. Harada, et al., Org. Chem. Front. 4 (2017) 1726–1730.
[21] C.M. Bertea, J.R. Freije, H. van der Woude, et al., Planta Med. 71 (2005) 40–47.
[22] C.F. Lee, L.X. Chen, C.Y. Chiang, et al., Angew. Chem. Int. Ed. 58 (2019) 18414–18418.
[23] S.W. Haynes, X. Gao, Y. Tang, C.T. Walsh, J. Am. Chem. Soc. 134 (2012) 17444–17447.
[24] S. Li, J.M. Finefield, J.D. Sunderhaus, et al., J. Am. Chem. Soc. 134 (2012) 788–791.
[25] Z. Liu, F. Zhao, B. Zhao, et al., Nat. Commun. 12 (2021) 4158.
[26] P. Kovacic, R. Somanathan, Oxid. Med. Cell. Longev. 3 (2010) 13–22.
[27] W. Cheng, M. Chen, M. Ohashi, Y. Tang, Angew. Chem. Int. Ed. 61 (2022) e202116928.